

CONF 8609190 -- 3

CONF-8609190--3

1

DE87 005976

P.-G. REINHARD ET AL

1. INTRODUCTION

Classical Mean-Field theories, e.g. Skyrme-Hartree-Fock, /QF78/, have proven to be a useful basis for static and dynamic properties of nuclei. It is interesting to investigate also a relativistic Mean-Field model where the nucleons obey the Dirac-equation and the forces are mediated by explicit mesonic degrees-of-freedom. In fact such a relativistic treatment is almost as old as classical models /MG72, Wa74/ and it has since been studied extensively; for a recent review see /SW85/.

In this contribution we look at the relativistic Mean-Field model from many aspects. First, we investigate the ability of the theory to describe nuclear ground-state properties /RR86/; this is done systematically by means of least-squares fits to experimental data, and, of course, we restrict this study to spherical nuclei in order to reduce the expenses. Second, we look at the properties of deformed nuclei within the relativistic approach; these are first exploratory calculations for light nuclei /Le86/. Third, we study dynamic properties for the example of a relativistic $^{16}\text{O} - ^{16}\text{O}$ collision /CR85/.

The paper is outlined as follows: In section 2 we explain the theory. In section 3, we explain the computation of observables. In section 4, we present the fits to (spherical) nuclear data. In section 5, we show the result of deformed calculations. And in section 6, we discuss the relativistic heavy-ion collision.

RELATIVISTIC MEAN-FIELD THEORIES AND NUCLEAR PROPERTIES

P.-G. REINHARD
Institut für Theoretische Physik
Universität
D-8520 Erlangen
West-Germany

M. RUFA, J. FINK, J. MARUHN, H. STÖCKER and W. GREINER
Institut für Theoretische Physik
Universität
D-6000 Frankfurt
West-Germany

S.Y. LEE, S. UMAR and M.R. STRAYER
Oak Ridge National Laboratory
Oak Ridge/ TN 37831, USA

R.Y. CUSSON
Duke University
Durham/NC 27706, USA

The nucleus is described as consisting out of relativistic nucleons and explicit mesonic degrees-of-freedom which are considered to be the relativistic generalisation of the Skyrme force. The meson-parameters can be adjusted such that the model gives an excellent description of spherical nuclear ground states. First axially symmetric deformed calculations are presented. Dynamic calculations of relativistic $^{16}\text{O} - ^{16}\text{O}$ scattering are also done; they show pronounced effects of the mesonic degrees-of-freedom.

MASTER

DISTRIBUTION OF THIS DOCUMENT IS UNLIMITED

EAC

RELATIVISTIC MEAN-FIELD THEORIES...

2. THE RELATIVISTIC MESON-FIELD MODEL

We want to describe the nucleus as a relativistic system consisting of nucleons which obey the Dirac equation, and of mesons which mediate the internucleon forces. From the many possible mesons we choose a few with simple internal quantum numbers (spin 0 or 1, isospin 0 or 1, no strangeness) and with low mass; these are

- an isoscalar-scalar (σ) meson field ϕ ,
- an isoscalar-vector (ω) meson field V_μ ,
- an isovector-vector (ρ) meson field R_μ ,
- and the photon field A_μ .

One misses the π -field in that list as well as the η -mesons. These are pseudoscalar mesons, and therefore they have vanishing expectation value for the ground state of nuclei and nuclear matter (unless parity were broken which is very unlikely). Thus pseudoscalar mesons will not contribute in a Mean-field approximation and we neglect them in the following.

We choose always the simplest coupling of the mesons, selected above, to the nucleons. For the scalar meson field we also include a cubic and quartic nonlinear self-coupling in order to give the model sufficient flexibility to describe nuclear response features /BB77/. Altogether the model Lagrangian density reads (in units $\hbar=c=1$)

$$\begin{aligned} \mathcal{L} = & \bar{\psi}(i\gamma^\mu \partial_\mu - m_N)\psi \\ & + \frac{1}{2}[(\partial^\mu \phi \partial_\mu \phi - m_\sigma^2 \phi^2) - g_\sigma \bar{\psi} \psi - \frac{1}{3}b_2 \phi^3 - \frac{1}{4}b_3 \phi^4] \\ & - \frac{1}{2}[(\partial_\nu V_\mu - \partial_\mu V_\nu)^2 \partial^\nu V^\mu - m_\omega^2 V_\mu V^\mu] - g_\omega V^\mu \bar{\psi} \gamma_\mu \psi \quad (1) \end{aligned}$$

P.-G. REINHARD ET AL

$$\begin{aligned} & - \frac{1}{2}[(\partial_\nu R_\mu - \partial_\mu R_\nu)^2 \partial^\nu R^\mu - m_\rho^2 R_\mu R^\mu] - \frac{1}{2}g_\rho R^\mu \bar{\psi} \gamma_\mu \tau \psi \\ & - \frac{1}{2}[(\partial_\nu A_\mu - \partial_\mu A_\nu)^2 \partial^\nu A^\mu] - \frac{1}{2}e A^\mu \bar{\psi} \gamma_\mu (1 + \tau_3) \psi \quad (1) \end{aligned}$$

where ψ is the nucleon field and $\bar{\psi} = \psi^\dagger \gamma_0$; the γ^μ are the usual Dirac matrices /BD 64/. The first line describes the free nucleon Lagrangian and the other lines are the meson Lagrangians with their couplings to the nucleons (and the self-couplings of the scalar meson). It is a formidable task to determine the full quantal dynamics of the Lagrangian (1). It would have to include all many-body-effects, namely

- self consistent field,
- exchange diagrams,
- two body correlations (ladder diagrams),
- core polarisation (bubble diagrams), etc,
- and all quantum field effects, namely
- vacuum polarisation,
- mass renormalisation,
- charge renormalisation, etc..

In fact, that is an almost impossible task; and it is useless as well, because we know that nucleons and mesons are not the basic constituents of matter. The Lagrangian (1) is to be considered as being just a phenomenological Lagrangian for a relativistic nuclear model and it makes most sense in connection with approximations.

We employ first the

Mean-Field approximation: $\hat{\phi} + \phi, \hat{V}_\mu + V_\mu,$

$$\hat{R}_\mu + R_\mu, \hat{A}_\mu + A_\mu, \quad (2)$$

RELATIVISTIC MEAN-FIELD THEORIES...

i.e. all meson fields are treated as classical c-number fields. Accordingly the nucleon currents become c-number currents, $\bar{\Psi}\Psi + \rho_S = \langle \bar{\Psi}\Psi \rangle$ etc, and the ground state expectation values $\langle \dots \rangle$ can be expressed by the nucleon single particle wave functions ψ_α , e.g.

$$\rho_S = \langle \bar{\Psi}\Psi \rangle = \sum_{-\infty}^{+\infty} \chi_\alpha \bar{\psi}_\alpha \psi_\alpha \quad (3)$$

where $\chi_\alpha = +\frac{1}{2}$ below the Fermi-energy and $\chi_\alpha = -\frac{1}{2}$ above the Fermi-energy. With the Mean-field approximation we retain from all the many-body effects only the self consistent field and from all quantum field effects just the vacuum polarisation. That is a most dramatic simplification of the task.

The vacuum polarisation is hard to evaluate since it involves a sum over a continuum of states, see the schematic plot of the nucleon spectrum in fig. 1. The vacuum polarisation is an accumulated effect from the infinity of negative-energy states /CH 77/. The predominant self-consistent field is build from the few occupied positive-energy bound states which correspond to the conventional nuclear shell model states. We come down to a manageable set of equations by neglecting the vacuum polarisation, i.e. we employ the

$$\text{No-Sea approximation: } \sum_{\alpha=-\infty}^{+\infty} \chi_\alpha \dots \rightarrow \sum_{\alpha=1}^A \dots \quad (4)$$

where all sums accumulating nucleon densities run over the shell model states only.

By variation of the model Lagrangian (1) and employing the Mean-field approximation (4) we obtain the coupled equations for the nucleon wave functions ψ_α and for the

P.-C. REINHARD ET AL

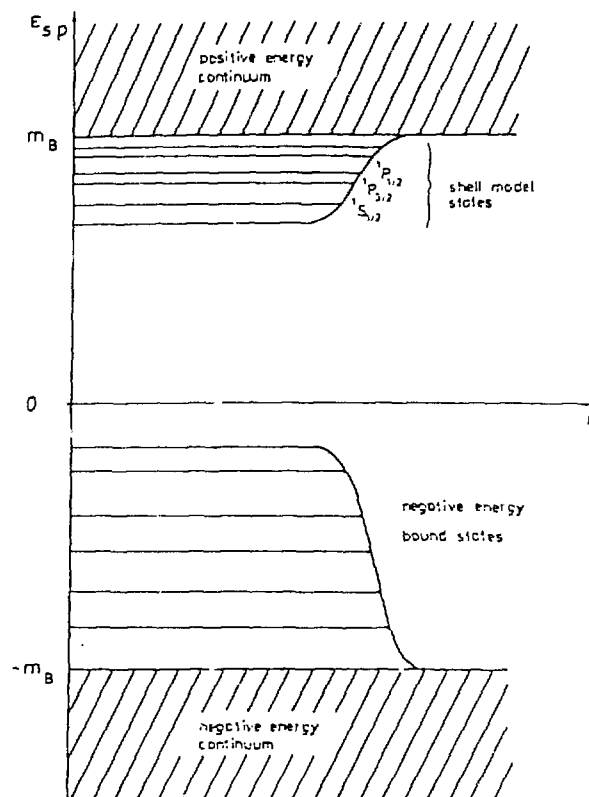


Fig. 1. Schematic spectrum of the Dirac equation for the nucleons. The positive energy bound state exhibit a one-to-one correspondence to the states of a classical nuclear shell model. This is indicated by denoting these states with the usual spectroscopic quantum numbers. The potential for negative energy states can also support bound states as indicated

RELATIVISTIC MEAN-FIELD THEORIES...

meson fields ϕ , V_μ , R_μ and A_μ :

$$i\gamma_0 \frac{\partial}{\partial t} \varphi_\alpha = (-i\gamma \cdot \nabla + m_N + g_S \phi + g_V V_\mu^\mu + \frac{1}{2} g_R R_\mu^\mu + \tau \gamma_\mu + e A_\mu \frac{1+\tau_3}{2} \gamma_\mu) \varphi_\alpha \quad (5a)$$

$$\left(\frac{\partial^2}{\partial t^2} - \Delta + m_S^2\right) \phi = -g_S \rho_S - b_2 \phi^2 - b_3 \phi^3, \quad \rho_S = \sum_{\alpha=1}^A w_\alpha \bar{\varphi}_\alpha \varphi_\alpha \quad (5b)$$

$$\left(\frac{\partial^2}{\partial t^2} - \Delta + m_V^2\right) V_\mu = +g_V \rho_\mu, \quad \rho_\mu = \sum_{\alpha=1}^A w_\alpha \bar{\varphi}_\alpha \gamma_\mu \varphi_\alpha \quad (5c)$$

$$\left(\frac{\partial^2}{\partial t^2} - \Delta + m_R^2\right) R_\mu = +\frac{1}{2} g_R \rho_\mu, \quad \rho_\mu = \sum_{\alpha=1}^A w_\alpha \bar{\varphi}_\alpha \gamma_\mu \tau \varphi_\alpha \quad (5d)$$

$$\left(\frac{\partial^2}{\partial t^2} - \Delta\right) A_\mu = e \rho_{p,\mu}, \quad \rho_{p,\mu} = \sum_{\alpha=1}^A w_\alpha \bar{\varphi}_\alpha \gamma_\mu \frac{1+\tau_3}{2} \varphi_\alpha \quad (5e)$$

Note that an occupation weight w_α has been implemented in the sums for the nucleon densities. This is to give the model the flexibility to describe also non-magic nuclei. In practice we are using a schematic pairing within the constant gap approach with a gap $\Delta = 11.2 \text{ MeV } A^{-1/2}$. For closed shell nuclei, of course, we set $w_\alpha = 1$ throughout. Note furthermore that proton- and neutron-wave-functions usually do not mix; then only the τ_0 -component in the isovector current ρ_μ exists and only the $R_{\tau_0,\mu}$ field component needs to be retained.

The eqs. (5) still embrace all possible applications. For dynamical calculations, e.g. of relativistic heavy ion collisions, they are to be treated to full extent. For static application, the eqs. (5) can be simplified:

P.-G. REINHARD ET AL

the meson fields are independent of time, thus $\frac{\partial^2}{\partial t^2} \phi = 0$ etc and the nucleon wave functions are stationary, thus $i \frac{\partial}{\partial t} \varphi_\alpha = \epsilon_\alpha \varphi_\alpha$ with ϵ_α being the single particle energy; furthermore the space-vector parts of meson fields vanish, i.e. only V_0, R_0, τ_0 and A_0 need to be treated. For spherical static calculation the problem becomes even simpler: the fields are rotational invariant, $\phi(r) \rightarrow \phi(|r|)$ etc, and the nucleon wave functions separate into radial function and spinor spherical harmonics.

Altogether the relativistic Meson-field model consists out of the Lagrangian (1) together with the approximations (2) and (4). Thus the Lagrangian is an effective Lagrangian for relativistic Mean-Field calculation. This is a similar situation as with the Skyrme force which is an effective force for classical nuclear Mean-field calculations: the structure of the Lagrangian is inspired by theoretical considerations; the parameters therein, however, are considered as being free parameters of the model to be adjusted to observable nuclear properties. The free parameters of the relativistic Lagrangian (1) are the meson-masses m_S, m_V and m_R and the couplings g_S, g_V, g_R, b_2 and b_3 . The photon coupling e is fixed to the known value by requiring that the nuclear Coulomb field has the right asymptotics. Due to the Mean-Field approximation (2) there is no nucleon-mass renormalisation and we can fix the experimental value

$$m_N = 938.9 \text{ MeV} \quad (6)$$

as an average of proton and neutron mass. The free model parameters are to be fixed by fits to observable nuclear ground-state properties. We make the experience, that the

RELATIVISTIC MEAN-FIELD THEORIES...

masses of the ω -meson and of the ρ -meson are rather insensitive to the data. Thus we fix them at nearly the OBEP values /Ho 81/

$$m_V = 780. \text{ MeV} \quad , \quad (7)$$

$$m_R = 763. \text{ MeV} \quad , \quad (8)$$

and we are left with the 6 free model parameters m_S , g_S , g_V , g_R , b_2 and b_3 to be adjusted.

3. THE GROUND-STATE OBSERVABLES

The solution of the eqs. (5) delivers meson fields and nucleon wave functions. From these we have to evaluate some observables in order to compare with experimental data. The most obvious observable is the total energy of the system. It can be derived from the Lagrangian (1) by standard techniques /BD 65/; this yields

$$\begin{aligned} E_{MF} = & \int d^3r \left\{ \frac{A}{\Omega} \left[\frac{1}{2} \sum_{\alpha} \bar{\psi}_{\alpha} \psi_{\alpha} \right] \right. \\ & + \frac{1}{2} \left[(\dot{\phi}^2 + \nabla\phi^2) + m_S^2 \phi^2 \right] + \frac{1}{3} b_2 \phi^3 + \frac{1}{4} b_3 \phi^4 \\ & - \frac{1}{2} \left[\dot{V}_{\mu}^2 + \nabla V_{\mu} \cdot \nabla V^{\mu} + m_V^2 V_{\mu}^2 \right] \\ & - \frac{1}{2} \left[\dot{R}_{\mu}^2 + \nabla R_{\mu} \cdot \nabla R^{\mu} + m_R^2 R_{\mu}^2 \right] \\ & \left. - \frac{1}{2} \left[\dot{A}_{\mu}^2 + \nabla A_{\mu} \cdot \nabla A^{\mu} \right] \right\} \end{aligned} \quad (9)$$

P.-G. REINHARD ET AL

For the static case one can omit again \dot{V}_{μ} , \dot{R}_{μ} and \dot{A}_{μ} , and let $i \frac{\partial}{\partial t} \psi_{\alpha} + \epsilon_{\alpha} \psi_{\alpha}$. The energy (9) is the contribution from the Mean-Field theory. If we determine the occupation numbers w_{α} by pairing we have to add the pairing energy. Finally we have to account for a spurious centre-of-mass motion of the nucleus in its own Mean-Field. This is done by subtracting a centre-of-mass correction to the energy

$$E_{c.m.} = \frac{\langle \hat{p}^2 \rangle}{2mA}$$

Altogether the total energy is composed from three pieces as

$$E_{total} = E_{MF} + E_{Pair} - E_{c.m.}$$

The energy is the only observable which can be derived consistently from a given effective Lagrangian (and the implied approximations). All other observable, as e.g. formfactors or transition moments, would need to know the exact transformation from an "ab initio" Lagrangian to the effective one, because the same transformation should be applied to the observable (which usually is a given "ab initio" object). This transformation includes all the neglected many body and quantum field effects (see previous section); they are often called correlations as it is everything beyond the Mean-Field approximation. We do not know this correlation-transformation since we just parametrize the effective Lagrangian. Thus the only solution we have is that we select observables which can be expected to be insensitive to correlations. We think that the bulk properties of the nuclear charge and mass distribution, as e.g. the radius, the surface thickness, or the quadrupole deformation, are such observables.

RELATIVISTIC MEAN-FIELD THEORIES...

Radius and surface thickness are derived from the charge formfactor of the nucleus. For the spherical calculations, the formfactor is obtained from the nucleon density (zero component of the vector current) by a Fourier-Bessel transformation

$$F_t(q) = 4\pi \int_0^{\infty} dr r^2 j_0(qr) \rho_{c,t}(r) \quad (12)$$

where $t = \text{proton}$ or $t = \text{neutron}$. The nuclear charge formfactor is obtained by folding in the proton- and neutron-formfactor /SS80/ and unfolding the spurious centre-of-mass motion /QF78,FR86/. The radius R is then given by the first zero of the charge formfactor

$$R = 4.493/q^{(1)} \quad , \quad F_c(q^{(1)}) = 0 \quad (13)$$

and the surface thickness σ is determined from the suppression of the first maximum compared to the formfactor of a hard sphere with radius R ,

$$\sigma^2 = \frac{2}{q_m^2} \log \left(\frac{3j_1(q_m R)}{q_m R F_c(q_m)} \right) \quad , \quad (14)$$

$$F_c(q_m) = 1 \text{ Maximum} \quad .$$

Note that the radius R is the diffraction radius and not the r.m.s. radius. It is more related to the box-equivalent radius and it has the advantage that the diffraction radius is most insensitive to correlation effects (folding does not shift the zeroes of F_c) /FV 82, RF 85/. Both Fourier components, $q^{(1)}$ for R and q_m for σ , occur at lower q and low q are less influenced by correlation effects than high q . Thus we hope that R and σ are appropriate observables for

P.-G. REINHARD ET AL

a Mean-Field theory.

The quadrupole moment is used as an observable for deformed calculations. It is

$$Q_{20} = \int d^3r r^2 Y_{20} \rho_0(r) / \int d^3r \rho_0(r) \quad (15a)$$

where ρ_0 is given by eq. (5c). The Q_{20} has dimensions fm^2 . The dimensionless quadrupole deformation is derived from Q_{20} by

$$\beta = \bar{\beta} \left(1 + \frac{5}{4n} \bar{\beta}^2 \right), \quad \bar{\beta} = \frac{4\pi}{5Ar^2} Q_{20} \quad (15b)$$

where r is the r.m.s. radius for the nucleus.

4. OPTIMISING GROUND STATE PROPERTIES OF SPHERICAL NUCLEI

The solution of the coupled field equations becomes fairly simple for the ground-state (static limit) of spherical nuclei. With the usual spherical representation /B064/ and employing the inverse gradient step /R82/ we have set up a very fast program. Such that one can afford extensive and systematic investigations of the model parameters.

As explained in Sect. 2, the model has the free parameters g_s , b_2 , b_3 , g_v , g_R , m_s , m_v and m_R . We want to adjust these parameters such that the model reproduces as good as possible measured ground state properties of nuclei: binding energies and formfactors. We do this by minimizing the squared deviation $\chi^2 = \sum_n (O_n^{\text{exp}} - O_n^{\text{theory}})^2 / \Delta O_n^2$ with respect to the parameters of the theory. Here the sum runs over all chosen observables O_n . In experimental data analysis the ΔO_n is the statistical error on the data. In our case, we cannot use just the experimental error because both observables, binding energy and formfactor, are measured with a much higher precision than any theory can reach. The systematical error is, so to say, too large. Therefore we insert for ΔO_n what we expect to be the ability of the theory to describe that observable O_n . This way we regulate the relative weights of the contributions.

In table 2 we show the selection of the observables, their experimental values and the adopted errors; their theoretical definition is outlined in section 3. The selection covers a wide range in mass number, and some isotopic trends by the isotopes of Ca and Sn. In contrast to similar fits of the Skyrme force /FR86/ we do not include any explicit information about the spin-orbit splitting. A relativistic theory should predict this properly without any further help.

TABLE 1

Nucleus	Energy [E_{total}] [MeV]	diffr. radius R [fm]	surface σ [fm]
^{16}O	- 127.6	2.777	0.839
^{40}Ca	- 342.1	3.845	0.978
^{48}Ca	- 416.0	3.964	0.881
^{58}Ni	- 506.5	4.356	0.911
^{90}Zr	- 783.9	5.040	0.957
^{116}Sn	- 988.7	5.537	0.947
^{124}Sn	-1.050.0	5.640	0.908
^{208}Pb	-1.636.4	6.806	0.900
adopted error	0.2%	0.5%	1.5%

Table 1: Selection of observables, their experimental values and their adopted errors.

The χ^2 is minimized by standard techniques /Be69/. We have performed the χ^2 -fits under some varying conditions, as explained below. The results for the achieved precision in E , R and σ are compiled in fig. 2. First we concentrate on the "standard fit" including all data and computing all observables as explained above (denoted by a full circle ●). The resulting parameters are: $m_s=488.176 \text{ MeV}=2.47805 \text{ fm}^{-1}$, $g_s=10.0409$, $b_2=13.3451 \text{ fm}^{-1}$, $b_3=-39.6023$, $g_v=12.9091$ and $g_D=9.6991$. The model is obviously capable to adjust a very good description of nuclear ground state properties, with an error of 0.35% in σ . This precision can compete with the quality of the best adjusted Skyrme forces /B082, FR86/. It is important to note that the nonlinear scalar self-couplings are needed to obtain this precision. A similar fit with fixed $b_2=0$ and $b_3=0$ yields an average error in E of 2%, in R of 1.4% and in σ of 23%. It is obvious that the surface σ is more critical in the fit than energy E and

RELATIVISTIC MEAN-FIELD THEORIES...

P.-G. REINHARD ET AL

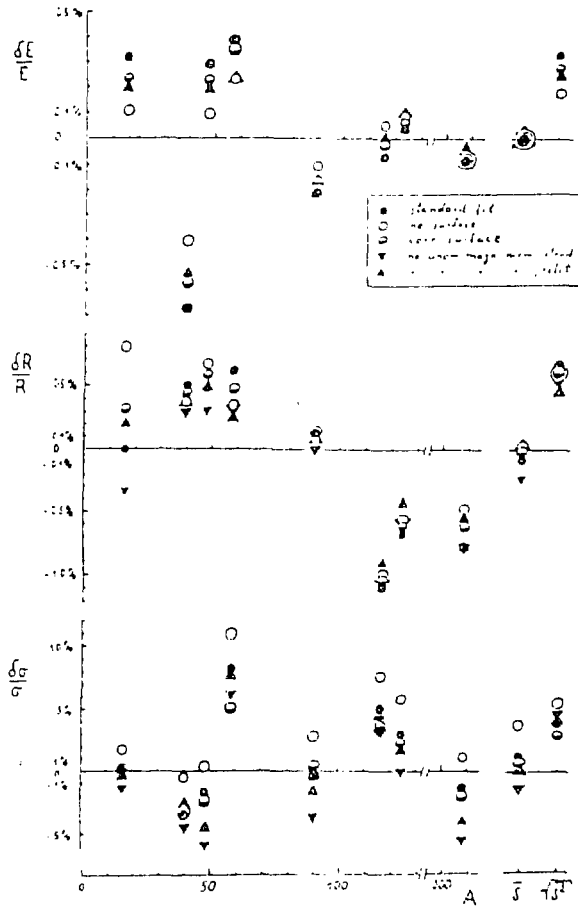


Fig. 2: The relative errors in E , R and σ for the eight fit nuclei, drawn versus mass number A . The extra column δ means the direct average of the deviation and δ^2 the mean-square error. The various fits are denoted by different symbols as explained in the above box.

radius R . To estimate its effect we have performed a fit which includes only E and R as data, see the open circles (\circ) in fig. 2. This allows to fit the energy E much better; for the radius R the effect is mixed with a slight overall improvement, and the surface thickness σ is, of course less well described. Note, however, that the quality of σ has only moderately worsened (from 3.5% to 5%) and that there is a systematic shift to smaller surfaces for all nuclei (see also the column δ in fig 2). The Mean-Field model seems to prefer steeper surfaces than observed in experiment.

And indeed it is well known that effects beyond the Mean-field approximation soften the surface, in particular the ground-state correlations due to nuclear collective vibrations /RF85/. The dominant effect on the surface thickness σ comes from the collective surface vibrations, the low lying 2^+ states. Their vibrational width and with it their effect on σ can be estimated from the $B(E2)$ value for the $0_1^+ \rightarrow 2_1^+$ transition /RF85/. We have corrected the experimental σ for that effect and performed the fit with the corrected data. This yields the half-filled circles (\ominus) in fig. 2. There is an overall improvement in the fit, in particular for the precision on σ . Note that this improvement comes mainly from the three nuclei with large surface vibration, namely ^{58}Ni , ^{116}Sn and ^{124}Sn . Further improvement is conceivable if one also accounts for the correlations from giant resonances. In any case we see that the fits exhaust the Mean-field model to the limits where correlation effects are inevitable.

Some other kind of correlations have already been implemented in the way the charge formfactor is composed: we fold in the proton and the neutron formfactor and we add

RELATIVISTIC MEAN-FIELD THEORIES...

the contribution of the nucleonic anomalous magnetic moment to the Coulomb field. The latter piece can be counted as a quantum field correlation effect (meson clouds). In order to investigate the influence of the anomalous magnetic moment we first have left out this contribution in a calculation with the "standard fit", given above; this yields the inverted triangles (∇) in fig. 2. Nothing changes in E , of course. There is systematic shift to larger radii and larger surfaces. In the whole, the precision of the observables has not suffered very much. It can be restored completely by fitting anew without the anomalous magnetic moment, see the triangles (\blacktriangle) in fig. 2. Here we have an example of a type of correlations which is just at the boundary of the precision of the model.

All fits show a similar tendency. The average error column 3 in fig 2, is adjusted to almost zero and thus the mean squared error, column 4, lives from the fluctuation about the average. Nevertheless there is some systematics in these fluctuations: the energy trend along isotopic chains cannot be fully reproduced (see here the example Ca and Sn, more in /RR86/), and there is an overall trend in R with A . Both unresolved trends hint that something is missing in the model. These will be some correlations; it is yet to be found out which ones.

It is interesting to look what the model predicts for quantities which have not been included fits. The most prominent of them are the properties of symmetric nuclear matter. We show them, together with the predictions of some other models, in table 2. The techniques of a least-squares fit provides us also with an estimate of the statistical error on the prediction; this is given, pars pro toto, for the "standard fit" in the table 2. Note that all the vari-

P.-G. REIKHARD ET AL

ations of the nonlinear relativistic model give virtually the same prediction which agrees fairly well with the classical models, Skyrme-Hartree-Fock and liquid drop; except for the effective mass m_N^*/m_N which comes out always very low in the relativistic models (including the rel. Brueckner-Hartree-Fock). The linear relativistic model ($b_2=0$, $b_3=0$) deviates strongly, in particular for energy E and incompressibility K . It is interesting to note that the relativistic B.H.F. calculations /BM86/ agree fairly well with the extrapolated Mean-Field predictions; except for the binding energy which seems to be a bit small.

TABLE 2

	E/A [MeV]	ρ_0 [fm^{-3}]	K [MeV]	m_N^*/m_N
Standard fit	16.20	0.1507	177.8	0.584
	± 0.05	± 0.0009	± 8	± 0.004
Fit with corr. σ	16.19	0.1502	190.	0.585
Fit without σ	16.17.	0.1493	209.	0.584
Fit without anom. magn. moment	16.20	0.1502	199.	0.584
Fit with $b_2=0, b_3=0$	17.04	0.1429	584.	0.529
Skyrme fit Z_0 /FR86/	15.81	0.1627	233.	0.783
Relativ. Brueckner	15.32	0.161	201.	0.57
H.F. /BM86/				
Liquid drop model	15.95	0.145	212.	-

Table 2: The bulk properties of symmetric nuclear matter at equilibrium for the various fits and for some other model. E/A is binding energy per particle, ρ_0 is the nucleon density, K is the compressibility, and m_N^*/m_N is the effective mass.

RELATIVISTIC MEAN-FIELD THEORIES...

It is not enough space here to outline other features of the model. We summarize them shortly, more details may be found in ref. /RRB6/. The full model predicts 6 MeV spin orbit splitting of the 1p-level in ^{16}O which is exactly the experimental value. This is the great advantage of the relativistic model compared to the classical models that the spin properties are automatically implied and that no further terms and parameters are needed to adjust them. Note, however, that only the full model gives this good description. The linear model fails badly predicting 11 MeV for the spin-orbit splitting in ^{16}O . There are two other features where the classical Mean-field models failed: the level density near the Fermi-energy is systematically too low, and the amplitude of the shell fluctuations on the nuclear charge density is by a factor 2-3 too large. We have looked at this in the relativistic model and find that they fail exactly the same way as the classical models do. These are very probably again effects which call for an inclusion of correlations.

Altogether we see that the relativistic model is as flexible and powerful as the classical Skyrme-Hartree-Fock description. It allows the same marvelous reproduction of nuclear ground-state data, and it shares many of the failures of the classical model, which all hint at correlations (beyond Mean-Field). However, it is clearly superior in predicting spin properties. Furthermore it provides a good basis for any application where relativistic wave functions are needed.

P.-G. REINHARD ET AL

5. DEFORMED STATIC CALCULATIONS

The success of the spherical applications of the model motivates to do the next step in evaluating nuclear properties: the evaluation of deformed ground states. Before we can harvest interesting results on the relativistic effects in deformation properties, we have to work out some involved numerical techniques.

TABLE 3

Nucleus	E (MeV)	r (fm)	β	comment
12C	-94.1	1.99	-0.005	
16O	-128.9	2.29	0.006	
16O	-120.6	2.31	0.003	grid 0.25 fm
16O	-119.9	2.32	-	spherical code
20Ne	-142.2	2.62	-0.54	
20Ne	-161.5	2.45	-0.20	various
20Ne	-166.4	2.54	0.42	initial
20Ne	-141.3	4.21	1.51	deformations
20Ne	-121.9	7.20	2.39	
24Mg	-208.9	2.56	-0.20	
40Ca	-373.8	3.06	0.002	
40Ca	-358.2	3.09	-	spherical code
48Ca	-490.4	3.18	-0.0003	
48Ca	-466.7	3.21	-	spherical code

Table 3.: Results of calculations with the linear parametrization of ref.2: $g_s=10.3$, $g_v=12.6$, $m_s=550$, $m_v=783$ and $m_\sigma=938$ MeV, including Coulomb force. If not commented otherwise an axial grid with a spacing of 0.5fm has been used. The β is the dimensionless quadrupole deformation. The r is the r.m.s. radius.

We represent the four components of the nucleon wave function and the meson fields on an axial space grid. In order

to avoid the fermion doubling /BMB3/ we have used shifted grids for the four different components of the wave functions, employing a shift by half a mesh spacing either in z-direction or in r-direction or in both directions. As in similar classical calculations /DK81/ we derive consistent field equations on the grid by first discretising the action on the grid and then performing the variation. The energy of the system is computed from the (discretized) action by standard techniques of field theory. We restrict all further considerations to the static case where all objects are time-independent and in particular where all space-vector parts of the vector fields vanish. In order to employ the well established iteration techniques of classical calculations /RC82/ we transform the Dirac equation into an effective Schroedinger equation (having an energy-dependent mass), and we use then the damped gradient iterations /RC82/ to find the (local) minima of the action. The details of the numerical procedure will be published elsewhere /Le86/.

In table 3 we show the results of the relativistic axially deformed calculations for various light nuclei. Here the old linear parametrisation of Walecka /Wa76/ has been used throughout, and the dimensionless quadrupole deformation is defined as in eq. (15). First we note that the "standard" spherical nuclei, namely 16O, 40Ca, and 48Ca, come out to be spherical; the remaining small deformation indicates the precision of the numerical representation. For 16O we have compared two grid spacings, the standard grid with 0.5fm and a finer grid with 0.25fm spacing. The residual deformation is much smaller on the finer grid. We see also a dramatic change in the binding energy. This is similar to classical calculation. The fine grid gives

already an excellent description as one sees from the comparison with the spherical results. Nevertheless we prefer to use the "coarse" grid with 0.5fm spacing for reasons of computing time. The overall effect is mainly an energy shift which may be estimated from comparing spherical and deformed results for 16O, 40Ca and 48Ca.

The interesting results are those for the deformed nuclei. 20Ne and 24Mg show substantial deformations and they are comparable to classical calculations /QF78/ and to data. For 12C we obtain negligible deformation. That is not so surprising because 12C is rather a soft nucleus than a deformed system, and the position of the actual deformation minima depend sensitively on the forces used. In fact, we know that the spin orbit splitting tends to restore sphericity and that the parametrisation used in table 3 has a large spin-orbit force.

For 20Ne we have explored the whole range of axially deformed local minima. This was achieved by starting the iteration from various differently deformed initial configurations. The prominent minimum comes out at $\beta = 0.42$ in accordance with classical results. The occurrence of a, less favorite, oblate minimum is also quite common. The next oblate and prolate deformations are a bit surprising. They may be due to the fact that we compute always closed shell nuclei (with proper reordering of course); a pairing force may smoothen some of these extremely deformed minima. The most prolate solution, however, may survive because it represents quite clearly a chain of five α -particles loosely bound to each other. This configuration may be an effect of the parametrisation which produces a rather large binding for the α -particle.

6. DYNAMICS OF ^{16}O - ^{16}O COLLISIONS

A relativistic Mean-Field model is a natural starting point for a microscopic description of energetic heavy-ion collisions. We have applied the model, as outlined in section 2, to time dependent calculations of ^{16}O - ^{16}O scattering /CR85/. For these first exploratory calculations we have used a slightly simplified Lagrangian: we omit the photon, the ρ -meson and the nonlinear self-couplings of the σ -meson, i.e. we use the linear model of ref /Wa72/. The parameters are given in the table caption of table 3.

A few technical explanations are necessary:

We represent the meson fields and the baryon wave functions on a three-dimensional ($24 \times 24 \times 24$) mesh in coordinate space. Quantities in momentum space are obtained by means of a fast Fourier transform method. We employ isospin-degenerate nucleon wave functions and treat the spin degrees of freedom in the usual four-component spinor formalism. Thus we propagate eight independent four-component wave functions for each ^{16}O nucleus. We use the relativistic static Hartree wave functions for each of the ^{16}O initial states. The nuclei are located at a separation distance of 10 fm from each other on the mesh, and are Lorentz boosted to the appropriate initial energy in the center-of-velocity frame. The time evolution for the baryon wave functions is done with a fifth-order predictor-corrector in momentum space and the meson equations are solved simultaneously by Green's functions techniques. With the above mesh, the momentum-space truncation occurs at about 2 GeV/c. As a test of the accuracy of our numerical techniques we evaluate the total energy at each time step in the evolution, and note that it is constant to better than 1×10^{-5} . We have also

evaluated the continuity equation at each point in time to further guarantee the correctness of our solutions.

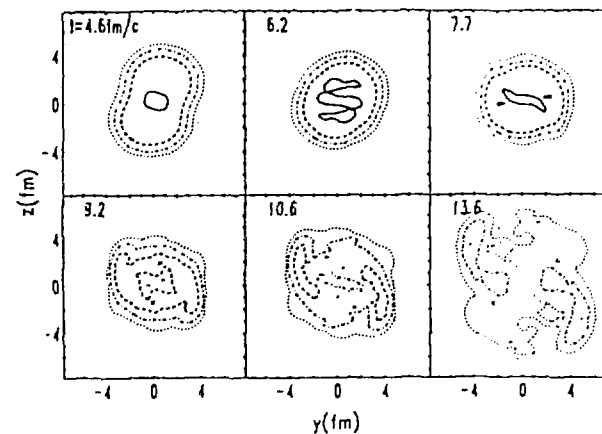


FIG. 3. Contour snapshots of the coordinate-space baryon density $\rho_B(x=0, y, z, t)$, in the scattering plane for $^{16}\text{O}(600A \text{ MeV}, b=2 \text{ fm}) + ^{16}\text{O}$. The maximum density is 0.29 fm^{-3} and is attained at 6 fm/c. The values of the density contours are as follows: solid curve, 0.26 fm^{-3} ; dashed curve, 0.10 fm^{-3} ; dot-dashed curve, 0.04 fm^{-3} ; large-dotted curve, 0.014 fm^{-3} ; and small-dotted curve, 0.005 fm^{-3} .

We have studied with this approach collisions of $^{16}\text{O}(E_{\text{lab}}=300, 600, \text{ and } 1200 \text{ MeV/nucleon}) + ^{16}\text{O}$ at various impact parameters. The time evolution is followed until the expanding matter reaches the edges of the mesh. We show in Fig. 3 the time evolution of the spatial baryon density for

RELATIVISTIC MEAN-FIELD THEORIES...

$E_{lab} = 600$ MeV/nucleon and $b = 2$ fm. The early time behavior in the approach is similar to that obtained by use of non relativistic TDHF. Subsequently, a compression zone and sideward flow develop (between $t = 6$ and 10 fm/c), after which the system proceeds to undergo spallation. This result can be contrasted with TDHF calculations at medium energies where projectilelike and targetlike fragments emerge after the reaction /SC80/. The sideward flow observed in the present approach resembles the large transverse-momentum transfer predicted by nuclear fluid dynamics /SM80/ and the VUU approach, /MS85/.

Both, the total spallation of the nuclei and the strong collective sideward flow, are caused by the meson field being own degrees-of-freedom. We find that the σ - and ω -meson fields develop strong out-of-phase oscillations in space and time, soon after the maximum compression point. The nucleons are deflected by these oscillations in fields. The strong space - time oscillations destroy the nucleon-nucleon binding and produce the spallation. The strongest meson fields are concentrated near the origin and that gives rise to the sideward flow.

Altogether the result of the relativistic Mean-Field dynamics are half-way between classical TDHF calculations and fluid dynamics. The mesonic degrees-of-freedom seem to produce effects which are usually expected from two-body correlations. They do not produce enough to reach the fluid dynamics limit. Probably some two-body correlations have still to be added. But certainly the relation between two - body effects and Mean-Field will be different in relativistic and in classical models. That is an interesting task for further studies.

P.-G. REINHARD ET AL

7. CONCLUSION

It has been shown that the relativistic Mean-Field theory is as capable in reproducing the bulk properties of nuclei as the classical Skyrme-Hartree-Fock model. A very precise description can be achieved with an error of 0.35% for the energies, of 0.6% for the radii, and of 3.9% for the surface thicknesses. Studying modifications of the model (surface vibrations, anomalous magnetic moments) we could show that the fit has exhausted the possibilities of a Mean-field model, and any step further needs to consider correlations of various sorts. We want to point out the advantage of relativistic over classical models that all spin properties (in particular the spin-orbit force) are implicit in the theory without requiring extra terms and extra parameters.

The relativistic model produces reasonable deformations roughly comparable to results of classical calculations. There are differences in detail which deserve further studies of model and force dependence of the deformation-energy surfaces.

The dynamic calculations show the most pronounced relativistic effect namely that the mesons, being now dynamical degrees-of-freedom of its own, produce part of the effects which are usually expected from two-body collisions. We observe complete spallation of the nuclei and pronounced collective sideward flow.

RELATIVISTIC MEAN-FIELD THEORIES...

REFERENCES

- /BB77/ J. BOGUTA, A.R. BODMER, Nucl. Phys., A 292 (1977) 414
 /BD64/ J.D. BJORKEN, S.D. DRELL, "Relativistic Quantum Mechanics", McGraw-Hill, New York 1964
 /BD65/ J.D. BJORKEN, S.D. DRELL, "Relativistic Quantum Fields", McGraw-Hill, New York, 1965
 /BE69/ P.R. BEVINGTON, "Data reduction and error analysis for the physical sciences", McGraw-Hill, New York 1969
 /BMB3/ C.H. BENDER, K.A. MILTON, D.M. SHARP, Phys. Rev. Lett. 51 (1983) 1815
 /BQB2/ J. BARTEL, P. QUENTIN, M. BRACK, C. GUET, M. B. HAKANSSON, Nucl. Phys., A 386 (1982) 79
 /Ch77/ S.A. CHIN, Ann. Phys., 83 (1977) 301
 /CR65/ R.Y. CUSSON, P.-G. REINHARD, J.J. MOLITORIS, M. STÜCKER, M.R. STRAYER, W. GREINER, Phys. Rev. Lett., 55 (1985) 2786
 /DKB1/ K.T.R. DAVIES, S.E. KODWIN, Phys. Rev., C 23 (1981) 2042
 /FR66/ J. FRIEDRICH, R.-G. REINHARD, Phys. Rev., C 33 (1986) 335
 /F182/ J. FRIEDRICH, N. VOEGLER, Nucl. Phys., A 373 (1982) 191
 /Ho81/ K. HOLLNDE, Phys. Rep., 68 (1981) 122
 /Le86/ S.J. LEE et al., to be published
 /MG72/ L.D. MILLER, A.E.S. GREEN, Phys. Rev., C5 (1972) 241
 /MS85/ J.J. MOLITORIS, H. STÜCKER, Phys. Rev., C 32 (1985) 346
 /QF78/ R. QUENTIN, M. FLOCARD, Ann. Rev. Nucl. Part. Sci., 28 (1978) 523
 /RC82/ P.-G. REINHARD, R.Y. CUSSON, Nucl. Phys., A 378 (1982) 418
 /RF85/ P.-G. REINHARD, J. FRIEDRICH, Z. Phys., A 321 (1985) 619
 /RR86/ P.-G. REINHARD, M. RUF, J. MARUHN, W. GREINER, J. FRIEDRICH, Z. Phys., A 323 (1986) 13
 /SC80/ H. STÜCKER, R.Y. CUSSON, J. MARUHN, W. GREINER, Z. Phys., A 294 (1980) 125
 /SM80/ H. STÜCKER, J. MARUHN, W. GREINER, Phys. Rev. Lett., 44 (1980) 725
 /SS80/ G.G. SIMON; Ch. SCHMITT, F. BORKOWSKI, V.M. WALTER, Nucl. Phys., A 333 (1980) 381
 /SWB5/ B.D. SEROT, J.D. WALECKA, Adv. Nucl. Phys., 16 (1985) 1
 /Wa74/ J.D. WALECKA, Ann. Phys., 83 (1974) 491

DISCLAIMER

This report was prepared as an account of work sponsored by an agency of the United States Government. Neither the United States Government nor any agency thereof, nor any of their employees, makes any warranty, express or implied, or assumes any legal liability or responsibility for the accuracy, completeness, or usefulness of any information, apparatus, product, or process disclosed, or represents that its use would not infringe privately owned rights. Reference herein to any specific commercial product, process, or service by trade name, trademark, manufacturer, or otherwise does not necessarily constitute or imply its endorsement, recommendation, or favoring by the United States Government or any agency thereof. The views and opinions of authors expressed herein do not necessarily state or reflect those of the United States Government or any agency thereof.